

Future Changes in Rainfall Extremes Associated with El Niño Projected by a Global 20-km Mesh Atmospheric Model

Akio Kitoh¹, and Hirokazu Endo²

¹University of Tsukuba, Tsukuba, Japan

²Meteorological Research Institute, Tsukuba, Japan

Abstract

A global high-resolution atmospheric general circulation model with grid size about 20 km is used to project future changes in rainfall extremes associated with El Niño at the end of the 21st century. In the future climate projections, hypothetical sea surface temperature (SST) is assumed where the interannual variability of SST remains same as in the present climate. The annual maximum 1-day precipitation total (R1d) over the western North Pacific is largely associated with tropical cyclone activity and positively correlated to the Niño3.4 SST anomalies. It is found that climatological mean R1d will only modestly increase in the western North Pacific in the future, but interannual variability of R1d will largely increase compared to the present due to enhanced association with El Niño. This implies an increasing risk of heavier rainfall events by global warming around the western North Pacific countries.

(Citation: Kitoh, A., and H. Endo, 2016: Future changes in rainfall extremes associated with El Niño projected by a global 20-km mesh atmospheric model. *SOLA*, **12A**, 1–6, doi:10.2151/sola.12A-001.)

1. Introduction

El Niño/Southern Oscillation (ENSO) is one of the biggest variability of the atmosphere-ocean coupled system, and influences most parts of the tropics and even some mid-latitudes. Present-day reproducibility of ENSO and its future change varies much among the models. By analysing 34 climate models participating in the Coupled Modeling Intercomparison Project phase 5 (CMIP5), Taschetto et al. (2014) find no consistent changes across the models in the location and magnitude of maximum sea surface temperature (SST) anomalies, frequency, or temporal evolution of El Niño events in a warmer world. IPCC (2013) assessed that natural modulations of the variance and spatial pattern of ENSO are so large in models that confidence in any specific projected change in its variability in the 21st century remains low. It is also assessed that ENSO will still be the most dominant year-to-year variations of the future tropical climate system and due to increased moisture availability, the associated precipitation variability on regional scales likely intensifies. Cai et al. (2015) showed that mean state change of the tropical Pacific will cause an increased frequency of extreme El Niño and La Niña events and an eastward shift of the ENSO rainfall teleconnections with a likely increased intensity. The CMIP5 models project a strengthening ENSO effect on the northwest Pacific and East Asia summer climate (Hu et al. 2014).

The western North Pacific is the most active region of tropical cyclones. There are numerous studies on the variability of tropical cyclones. Under the global warming, global maximum wind speed and precipitation rates are projected to increase (IPCC 2013). The ENSO is known to affect the western North Pacific tropical cyclone (typhoon) activity in its location (Takaya et al. 2010) and intensity (Camargo and Sobel 2005). Therefore, changes in both ENSO and tropical cyclones on local precipitation in a warmer

world should be investigated to assess changes in natural hazards to cope with possible risk increases.

A global high-resolution atmospheric general circulation model with grid size about 20 km is used to project future changes in rainfall extremes associated with El Niño at the end of the 21st century. As reliable projections of future ENSO characteristics are not available, we use hypothetical SST in the future climate projections where the interannual variability of SST is assumed to remain as in the present climate. This strategy is used to assess future changes in weather and climate extremes including tropical cyclones (Murakami et al. 2011, 2012) and heavy precipitation (Kitoh et al. 2009; Kitoh and Endo 2016) as well as changes in teleconnections such as the ENSO-forced Pacific-North Pacific pattern (Zhou et al. 2014).

2. Model and experiment

2.1 MRI AGCM

We used a global 20-km mesh Meteorological Research Institute (MRI) atmospheric general circulation model (AGCM) version 3.2 (MRI-AGCM3.2, Mizuta et al. 2012). The 20-km mesh version uses a triangular truncation at wave number 959 (T_1959) in the horizontal, which has 1920×960 grid points. There are 64 layers in the vertical with a top at 0.01 hPa. For cumulus parameterization scheme, a new mass-flux type scheme (Yoshimura et al. 2015) is used.

This model has superiority than the previous version in reproducing global distribution of strong tropical cyclones (TC) such as categories 4 and 5 (Murakami et al. 2012). In a warmer climate, genesis frequency of TC is projected to significantly decrease in the western North Pacific and South Pacific, and increase in the tropical central Pacific (Murakami et al. 2012). Endo et al. (2012) showed an increase in extreme precipitation in South Asia and Southeast Asia in future climate. Kitoh and Endo (2016) further investigated future changes in precipitation extremes. They found that South Asia is the region of the largest extreme precipitation increase, while heavy precipitation increases in all regional domains even where mean precipitation decreases.

2.2 Experiment method

The present climate simulation used the observed interannually varying monthly mean SST and sea-ice concentration during 1979–2003 based on the HadSST1.1 data (Rayner et al. 2003). Two 25-year ensemble simulations were made from different atmospheric initial conditions, thus we have 50-year present-day simulation data.

For the future climate (2075–2099), the boundary SST data were prepared by superposing the future change in the multi-model ensemble of SST projected by CMIP5 models to the present-day observed SST. See Mizuta et al. (2008) for the details. In order to assess the uncertainty in projections, we made other three simulations with different SST spatial patterns. Three SST patterns are obtained by a cluster analysis of 28 CMIP5 RCP8.5 experiments (Mizuta et al. 2014): cluster 1 is characterized by a nearly uniform warming in the both hemispheres, cluster 3 is dominated by a larger warming in the Northern Hemisphere than in the Southern Hemisphere, and cluster 2 shows a larger warming over the central equatorial Pacific (El Niño-like pattern). Overall, four-member 25-year simulations were performed for the future,

Corresponding author: Akio Kitoh, Faculty of Life and Environmental Sciences, University of Tsukuba, 1-1-1 Tennodai, Tsukuba, Ibaraki 305-8572, Japan. E-mail: kito.akio.ff@u.tsukuba.ac.jp. ©2016, the Meteorological Society of Japan.

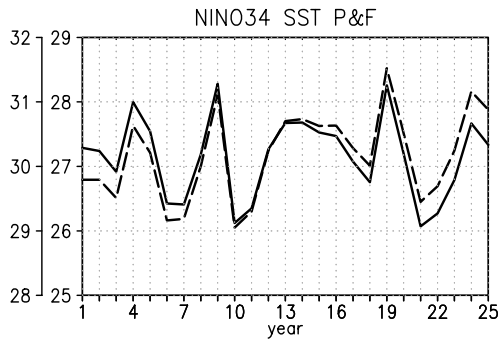


Fig. 1. Time-series of annual mean Niño3.4 SST ($^{\circ}\text{C}$). Solid line: present-day experiment for 1979–2003. Dash line: future experiment for 2075–2099.

resulting in 100-year data for future climate.

Kitoh and Endo (2016) investigated projected changes in regional precipitation extremes such as annual maximum 5-day precipitation total (R5d) and annual maximum 1-day precipitation total (R1d) over 22 regional land domains using the above ensemble simulation data, showing an increase in all regional domains, even where mean precipitation decreases. They also noted that different SST patterns resulted in large precipitation changes in some domains, possibly related to changes in large-scale circulations in the tropical Pacific.

Figure 1 shows the time-series of the prescribed mean Niño3.4 SST for the present and the future climate experiments. For clarity, annual mean values are shown, although monthly mean SST is used for the experiments. The 25-year mean difference is 3.03°C . Years of warm SST at year 4 (1982), year 9 (1987), year 19 (1997), and year 24 (2002) are clearly seen in the present climate experiment. Due to our experiment strategy, the same peaks are found in the future climate experiment. It is also noted that a linear trend in

the future period (0.91°C for 2075–2099) is larger than that in the present (-0.13°C for 1979–2003).

2.3 Observation data

In order to investigate precipitation extremes associated with ENSO, we use daily precipitation data. For observed precipitation data, we used Tropical Rainfall Measuring Mission (TRMM) 3B42 product in version 6 (Huffman et al. 2007), which covers 1998–2013. The TRMM data resolution is 0.25 degree and is very close to the model resolution.

For the observed TC tracks, we used International Best Track Archive for Climate Stewardship (IBTrACS) v03r06 (Knapp et al. 2010).

3. Present-day R1d associated with El Niño and tropical cyclones

MRI-AGCM3.2 shows good skill in simulating monsoon circulations and precipitation. The model also reproduces various characteristics of TC such as their intensity and global distribution (Mizuta et al. 2012). Kitoh and Endo (2016) showed that the 20-km mesh MRI-AGCM3.2 has good skill in reproducing precipitation extremes such as R1d in its present-day simulation.

Figure 2a shows the model climatology of R1d based on 50-year simulations corresponding to the 25-year period 1979–2003 (two ensembles with different atmospheric initial conditions). Note that all figures in the portrait format are drawn with 1 degree by 1 degree box averaging for visual easiness. Observation is given in Fig. 3a, which shows large R1d over the western Tropical Pacific and South China Sea, the Bay of Bengal, South Pacific Convergence Zone (SPCZ) and Inter-Tropical Convergence Zone (ITCZ). The 20-km mesh MRI-AGCM3.2 well reproduces spatial distribution as well as intensity of R1d compared with TRMM 3B42 data, although the model overestimates R1d over SPCZ and ITCZ. Area average R1d over 50°S – 50°N , 0° – 360° is 74.5 mm by the model, which is close to the observation (76.7 mm).

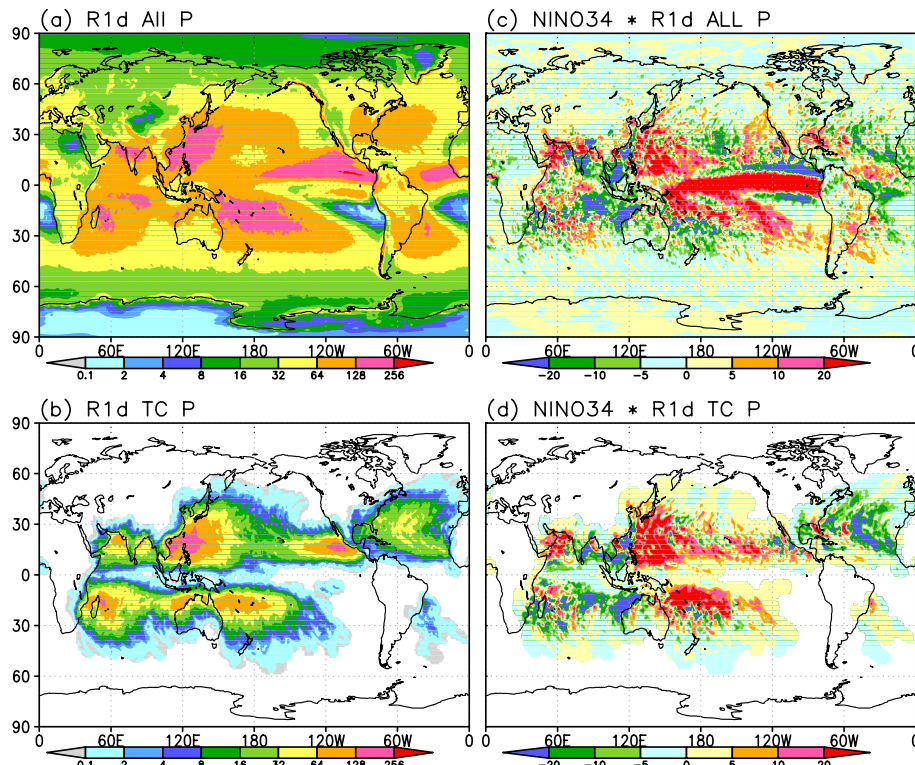


Fig. 2. Model climatology of the 20-km mesh MRI-AGCM3.2 for 1979–2003 of (a) R1d (mm), (b) R1d (mm) associated with tropical cyclones, (c) regression coefficients of R1d (mm) on Niño3.4 SST anomalies, and (d) regression coefficients of R1d (mm) associated with tropical cyclones on Niño3.4 SST anomalies. All figures are drawn by 1 degree \times 1 degree box averaging for visual easiness.

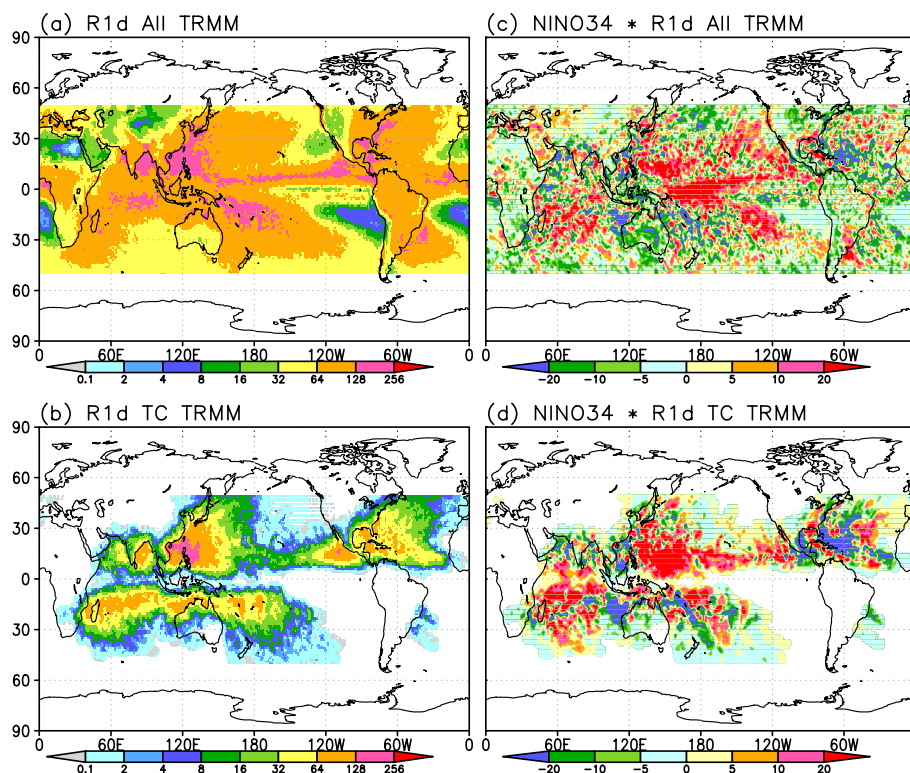


Fig. 3. Same as Fig. 2 except for the TRMM3B42 climatology for 1998–2013.

Heavy precipitation events in the tropics often occur associated with TC. We define TC-associated precipitation as that within a 500 km radius of TC centers because precipitation concentrates within a 5-degree radius around the TC centers (Kamahori 2012). As TC track data is available every 6 hours, calculation is made 6 hourly, and then accumulated daily precipitation is used to calculate TC-associated R1d. The criteria defining simulated TC are model-dependent in such a way that the present-day global annual mean TC number matches the observed number (84 per year) as shown in Murakami et al. (2012). In our definition, in years when TC does not exist within a 500 km radius of a given grid, TC-associated R1d becomes zero.

Figures 2b and 3b show that the 20-km mesh MRI-AGCM3.2 reproduces well the observed TC-associated R1d quantitatively. The ratio of the TC-associated R1d to the total R1d is greater than 80% over the western Pacific (the Philippines Sea and the South China Sea), off Mexico, northwest of Australia and east of Madagascar. There exist the years in which non-TC-associated rainfall contributes the R1d. Over the western Pacific, simulated TC-associated R1d is displaced northward compared to the observation. This may be related to the model's bias of a northward shift of typhoons (Murakami et al. 2012).

Next we investigate interannual variations of precipitation extremes associated with El Niño. Figure 2c shows regression coefficients of R1d on Niño3.4 SST anomalies. Here annual mean data in calendar year is used because R1d is calculated in an annual basis. As is well known, total precipitation anomaly in El Niño years is positive over the central equatorial Pacific and ITCZ in the eastern Pacific, and is negative over the western Pacific and maritime continent. This feature is well reproduced by the model (not shown). Simulated spatial regression map of R1d on Niño3.4 SST anomalies is overall similar to that of total precipitation, except for the western Pacific where R1d is positively correlated to Niño3.4 SST anomalies (Fig. 2c). This feature is also seen in the observed SST data for a period 1998–2013 (Fig. 3c), although a strict comparison cannot be made because of different data periods between the observation and the model.

Positive R1d anomalies over the western Pacific in El Niño

years come from heavy precipitation associated with TC. Figure 2d shows the regression coefficients of TC-associated R1d on Niño3.4 SST anomalies in the present-day experiment. Simulated TC-associated R1d in El Niño years is large positive to the east of the Philippines while negative in the South China Sea. It is also positive over the oceans northeast of Australia, while negative northwest of Australia. Over the Indian Ocean, it is positive over the western Indian Ocean and negative over the eastern Indian Ocean. Simulated TC-associated R1d in El Niño years is generally negative in the North Atlantic Ocean. Most of these features, in particular large contribution of TC for heavy precipitation in the western North Pacific, are seen in the observation (Fig. 3d).

4. Future changes

Here we investigate future changes in R1d, TC-associated R1d, and their regressions on Niño3.4 SST anomalies. R1d in the future climate will increase almost everywhere (Fig. 4a). Global average R1d increases about 25% from 61.6 mm to 77.5 mm. As the global annual mean surface air temperature increases 3.49°C in this experiment, the rate of R1d change is 7.4%/°C, which is close to the change of saturated vapor pressure by the Clausius-Clapeyron relationship.

Large R1d change is projected over the central-eastern equatorial Pacific and the equatorial Atlantic Ocean. India, central China, Sahel, equatorial South America and southern Brazil are the region of large R1d increases over land. The change is not significant over the western North Pacific. Future R1d is projected to decrease in some regions such as the South China Sea, the south-eastern Pacific Ocean and the southern Atlantic Ocean. The latter two regions correspond to the oceanic regions where climatological R1d is small (Fig. 2a). Similar to the spatial pattern of the total precipitation changes, which roughly follows the “wet-gets-wetter” (Held and Soden 2006) or “warmer-gets-wetter” pattern (Xie et al. 2010; Chadwick et al. 2013), future changes in R1d also follow the climatological R1d pattern (Fig. 2a). The exception is small change or reduction of R1d over the western North Pacific where

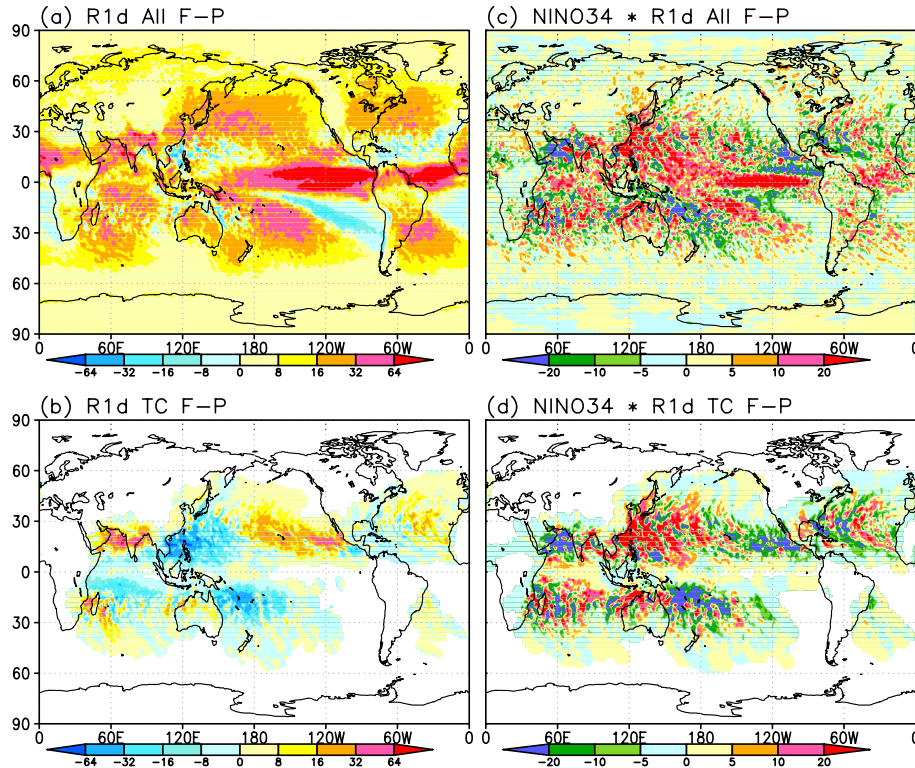


Fig. 4. Same as Fig. 2 except for the differences between the future (2075–2099) and the present (1979–2003).

the present-day R1d is large climatologically. This peculiar change may be related to changes in TC activity there.

Murakami et al. (2012) investigated the TC changes by the MRI-AGCM3.2 using the mean SST warming by the CMIP3 models under the SRES A1B scenario. They found a 15% decrease of global TC number at the end of the 21st century compared to the present-day conditions. Regionally, they noted a decrease of TC frequency in the western North Pacific and in the South Pacific Ocean, and a marked increase in the central Pacific. Using the same experiment results, Murakami et al. (2013a, 2013b) discussed physical mechanisms and found that changes in large-scale environmental conditions are responsible to regional TC genesis frequency changes.

In our experiment, the global TC genesis number is projected to decrease by 24%. A larger reduction in TC number than that in Murakami et al. (2012) is consistent with a larger warming in our experiment as our experiment is based on the RCP8.5 scenario.

Figure 4b shows the changes of TC-associated R1d in the future. The TC-associated R1d is projected to decrease in the western North Pacific, off the east of Australia, and tropical Indian Ocean. It is projected to increase near Hawaii, northern Indian Ocean. In other regions, changes are not statistically significant. This spatial pattern of TC-associated R1d change resembles the TC density change in the future (Fig. 5). Therefore, less activity of TCs in the western North Pacific in the future climate may have resulted in decreased TC-associated R1d.

Next we investigate R1d changes associated with El Niño (Fig. 4c). Regression coefficients of R1d on Niño3.4 SST anomalies are projected to increase over the northwestern Pacific, the equatorial Pacific and SPCZ. They will decrease off Mexico and off the east of Australia. Generally, the present-day pattern (Fig. 2c) is enhanced in the future climate, but statistical significance of changes in regression is low because of large interannual variability and small samples. There are some regional differences. For example, the positive anomalies in the South China Sea (Fig. 4c) imply weaker regressions in the future climate as compared to large negative regression coefficients in the present climate (Fig. 2c).

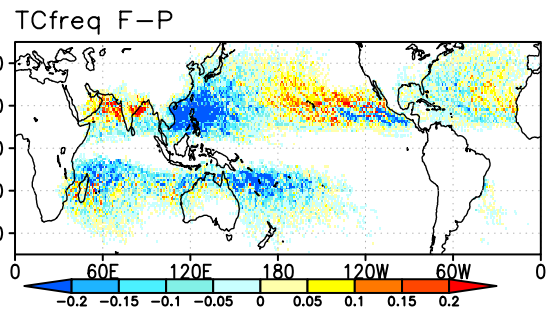


Fig. 5. Difference of tropical cyclone density (number per 25 years in each grid) by the 20-km mesh MRI-AGCM3.2 between the future (2075–2099) and the present (1979–2003).

In the present climate, TC-associated precipitation is particularly large in the western North Pacific in El Niño years (Fig. 2d). In the future climate, this TC-associated precipitation in El Niño years will become much stronger (Fig. 4d). On the other hand, changes in regression coefficients of TC-associated precipitation to Niño3.4 SST are negative over SPCZ and the Arabian Sea, and are positive over the Bay of Bengal and the southern Indian Ocean, tending to weaken the present-day relationship.

We have noted that R1d over the western North Pacific is very large in the present climate, but does not increase much in the future climate. Over there, TC-associated R1d actually decreases. Figure 6 shows the time-series of R1d averaged over the western North Pacific ($120^{\circ}\text{E}–180^{\circ}\text{E}$, $0^{\circ}\text{N}–25^{\circ}\text{N}$) for the present and the future. Here both the total R1d and TC-associated R1d are shown. The area average R1d increases by 11% from 106.8 mm to 118.5 mm, which is far less than the global mean R1d change (25%). In this region, the TC-associated R1d decreases by 25% from 52.4 mm to 39.4 mm, related to the TC density decrease by 47%.

On the other hand, interannual variability (denoted as standard deviations) increases both for total R1d and TC-associated R1d. A

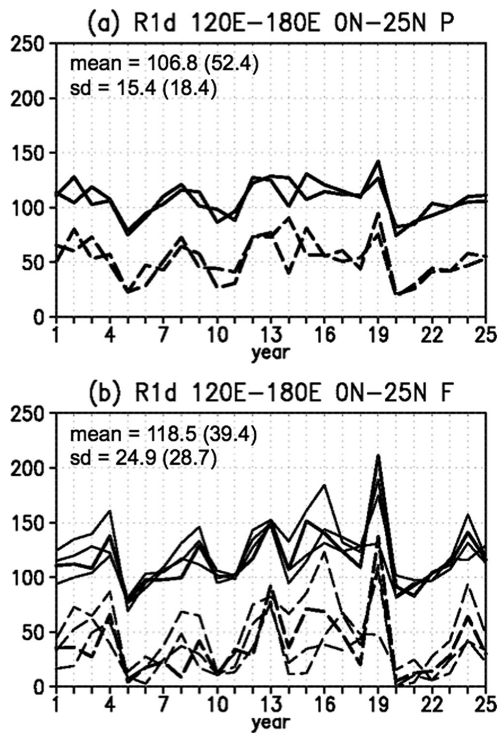


Fig. 6. Time-series of R1d (mm) averaged over the western tropical Pacific (120°E–180°E, 0°N–25°N) for (a) the present (1979–2003) and (b) the future (2075–2099). For the future, CMIP5 multi-model mean SSTA experiment is denoted by a thick line, while three cluster experiments are denoted by thin lines. Solid lines denote R1d, while dashed lines denote R1d associated with tropical cyclones. Values of 25-year average and its interannual standard deviation of R1d are shown in the upper left corner, while values of R1d associated with tropical cyclones are shown within brackets.

large increase is found in year 19, which corresponds to El Niño year (1997). The same is true for other three El Niño years (year 4, 13 and 24), but not so in year 9.

5. Summary

A global 20-km mesh MRI-AGCM is used to project future changes in rainfall extremes associated with ENSO and TC. About 3°C warming in SST is given in future scenario, embedded on the same interannually varying SST to the present.

Rainfall extremes such as R1d are projected to increase in the future warmer world, with larger increase over the regions where it is climatologically large. The exception is the western North Pacific where there is only small change or even reduction of R1d is projected. This is mainly related to a decrease of TC frequency in this region.

For interannual variability, R1d over the western North Pacific is larger in El Niño years than in other years. This is related with variability of TC activity. In the future warmer climate, mean R1d in the western North Pacific does not change much, but interannual variability of R1d greatly increases associated with ENSO. Therefore heavy precipitation such as once in a 10-year event can largely increase. This implies a drastic increase in risk of heavy-rainfall induced disasters under by global warming over the western Pacific countries. As non-inclusion of air-sea interaction may affect magnitude of precipitation (Kitoh and Arakawa 1999; Zou and Zhou 2016), more research is needed for quantitative discussions. It is also noted that statistical significance of changes in regression is low. One of the reasons is small sample size of the experiment, so that a large ensemble experiment is needed.

Acknowledgements

This work was conducted under the Development of Basic Technology for Risk Information on Climate Change of the SOUSEI Program of the Ministry of Education, Culture, Sports, Science, and Technology (MEXT) of Japan. The calculations were performed on the Earth Simulator of the Japan Agency for Marine-Earth Science and Technology.

Edited by: M. Sugi

References

- Cai, W., A. Santoso, G. Wang, S.-W. Yeh, S.-I. An, K. M. Cobb, M. Collins, E. Guilyardi, F.-F. Jin, J.-S. Kug, M. Lengaigne, M. J. McPhaden, K. Takahashi, A. Timmermann, G. Vecchi, M. Watanabe, and L. Wu, 2015: ENSO and greenhouse warming. *Nature Climate Change*, **5**, 849–859.
- Camargo, S. J., and A. H. Sobel, 2005: Western North Pacific tropical cyclone intensity and ENSO. *J. Climate*, **18**, 2996–3006.
- Chadwick, R., I. Boutle, and G. Martin, 2013: Spatial patterns of precipitation change in CMIP5: Why the rich do not get richer in the tropics. *J. Climate*, **26**, 3803–3822.
- Endo, H., A. Kitoh, T. Ose, R. Mizuta, and S. Kusunoki, 2012: Future changes and uncertainties in Asian precipitation simulated by multi-physics and multi-sea surface temperature ensemble experiments with high-resolution Meteorological Research Institute atmospheric general circulation models (MRI-AGCMs). *J. Geophys. Res.*, **117**, D16118, doi:10.1029/2012JD017874.
- Held, I. M., and B. J. Soden, 2006: Robust responses of the hydrological cycle to global warming. *J. Climate*, **19**, 5686–5699.
- Hu, K., G. Huang, X.-T. Zheng, S.-P. Xie, X. Qu, Y. Du, and L. Liu, 2014: Interdecadal variations in ENSO influences on Northwest Pacific-East Asian early summertime climate simulated in CMIP5 models. *J. Climate*, **27**, 5982–5998.
- Huffman, G. J., R. F. Adler, D. T. Bolvin, G. Gu, E. J. Nelkin, K. P. Bowman, Y. Hong, E. F. Stocker, and D. B. Wolff, 2007: The TRMM multi-satellite precipitation analysis: Quasi-global, multi-year, combined-sensor precipitation estimates at finer scale. *J. Hydrometeorol.*, **8**, 38–55.
- IPCC, 2013: *Contribution of Working Group I to the Fifth Assessment Report of the Intergovernmental Panel on Climate Change, Climate Change 2013: The Physical Science Basis*, Stocker, T. F., D. Qin, G.-K. Plattner, M. Tignor, S. K. Allen, J. Boschung, A. Nauels, Y. Xia, V. Bex, and P. M. Midgley, Eds., Cambridge University Press, Cambridge, United Kingdom and New York, NY, USA, 1535 pp.
- Kamahori, H., 2012: Mean features of tropical cyclone precipitation from TRMM/3B42. *SOLA*, **8**, 17–20.
- Kitoh, A., and O. Arakawa, 1999: On overestimation of tropical precipitation by an atmospheric GCM with prescribed SST. *Geophys. Res. Lett.*, **26**, 2965–2968.
- Kitoh, A., and H. Endo, 2016: Changes in precipitation extremes projected by a 20-km mesh global atmospheric model. *Weather and Climate Extremes*, **11**, 41–52.
- Kitoh, A., T. Ose, K. Kurihara, S. Kusunoki, M. Sugi, and KAKUSHIN Team-3 Modeling Group, 2009: Projection of changes in future weather extremes using super-high-resolution global and regional atmospheric models in the KAKUSHIN Program: Results of preliminary experiments. *Hydrol. Res. Lett.*, **3**, 49–53.
- Knapp, K. R., M. C. Kruk, D. H. Levinson, H. J. Diamond, and C. J. Neumann, 2010: The International Best Track Archive for Climate Stewardship (IBTrACS): Unifying tropical cyclone best track data. *Bull. Amer. Meteor. Soc.*, **91**, 363–376.
- Mizuta, R., Y. Adachi, S. Yukimoto, and S. Kusunoki, 2008: Estimation of future distribution of sea surface temperature and sea ice using CMIP3 multi-model ensemble mean. *Tech. Rep. Meteor. Res. Inst.*, **56**, 28pp.

- Mizuta, R., H. Yoshimura, H. Murakami, M. Matsueda, H. Endo, T. Ose, K. Kamiguchi, M. Hosaka, M. Sugi, S. Yukimoto, S. Kusunoki, and A. Kitoh, 2012: Climate simulations using MRI-AGCM3.2 with 20-km grid. *J. Meteor. Soc. Japan*, **90A**, 233–258.
- Mizuta, R., O. Arakawa, T. Ose, S. Kusunoki, H. Endo, and A. Kitoh, 2014: Classification of CMIP5 future climate responses by the tropical sea surface temperature changes. *SOLA*, **10**, 167–171.
- Murakami, H., B. Wang, and A. Kitoh, 2011: Future change of western North Pacific typhoons: Projections by a 20-km-mesh global atmospheric model. *J. Climate*, **24**, 1154–1169.
- Murakami, H., Y. Wang, H. Yoshimura, R. Mizuta, M. Sugi, E. Shindo, Y. Adachi, S. Yukimoto, M. Hosaka, S. Kusunoki, T. Ose, and A. Kitoh, 2012: Future changes in tropical cyclone activity projected by the new high-resolution MRI-AGCM. *J. Climate*, **25**, 3237–3260.
- Murakami, H., M. Sugi, and A. Kitoh, 2013a: Future changes in tropical cyclone activity in the North Indian Ocean projected by high-resolution MRI-AGCMs. *Climate Dyn.*, **40**, 1949–1968.
- Murakami, H., B. Wang, T. Li, and A. Kitoh, 2013b: Projected increase in tropical cyclones near Hawaii. *Nature Climate Change*, **3**, 749–754.
- Rayner, N. A., D. E. Parker, E. B. Horton, C. K. Folland, L. V. Alexander, D. P. Rowell, E. C. Kent, and A. Kaplan, 2003: Global analyses of sea surface temperature, sea ice, and night marine air temperature since the late nineteenth century. *J. Geophys. Res.*, **108**, 4407, doi:10.1029/2002JD002670.
- Takaya, Y., T. Yasuda, T. Ose, and T. Nakaegawa, 2010: Predictability of the mean location of typhoon formation in a seasonal prediction experiment with a coupled general circulation model. *J. Meteor. Soc. Japan*, **88**, 799–812.
- Taschetto, A. S., A. Sen Gupta, N. C. Jourdain, A. Santoso, C. C. Ummerhofer, and M. H. England, 2014: Cold tongue and warm pool ENSO events in CMIP5: Mean state and future projections. *J. Climate*, **27**, 2861–2885.
- Xie, S.-P., C. Deser, G. A. Vecchi, J. Ma, H. Teng, and A. T. Wittenberg, 2010: Global warming pattern formation: Sea surface temperature and rainfall. *J. Climate*, **23**, 966–986.
- Yoshimura, H., R. Mizuta, and H. Murakami, 2015: A spectral cumulus parameterization scheme interpolating between two convective updrafts with semi-Lagrangian calculation of transport by compensatory subsidence. *Mon. Wea. Rev.*, **143**, 597–621.
- Zhou, Z.-Q., S.-P. Xie, X.-T. Zheng, Q. Liu, and H. Wang, 2014: Global warming-induced changes in El Niño teleconnections over the North Pacific and North America. *J. Climate*, **27**, 9050–9064.
- Zou, L., and T. Zhou, 2016: Future summer precipitation changes over CORDEX-East Asia domain downscaled by a regional ocean-atmosphere coupled model: A comparison to the stand-alone RCM. *J. Geophys. Res. Atmos.*, doi:10.1002/2015JD024519.

Manuscript received 24 February 2016, accepted 13 April 2016
SOLA: <https://www.jstage.jst.go.jp/browse/sola/>